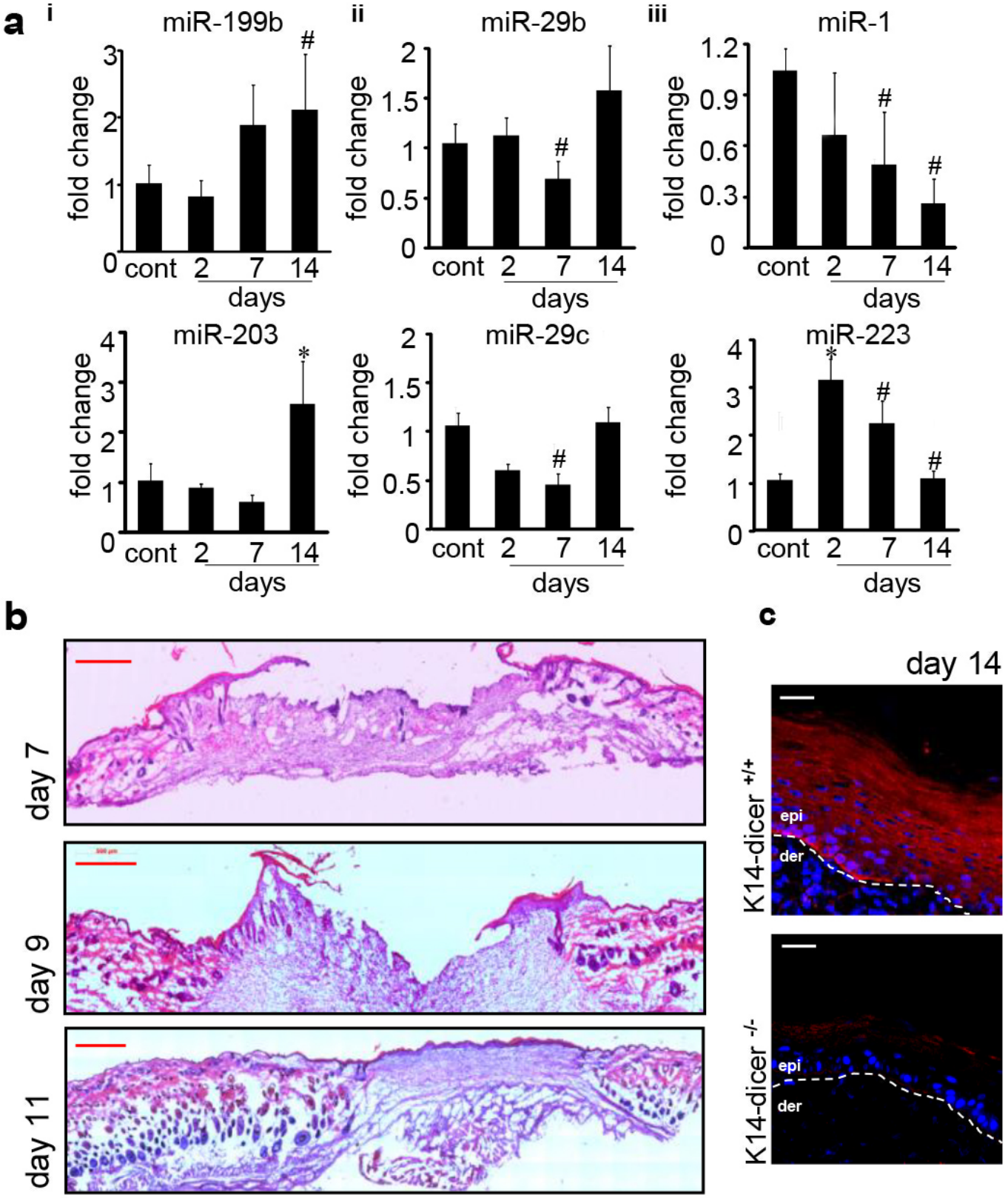

Figure S1: (a) Quantitative PCR analysis of different miRNAs from 3 different clusters at different time points post wounding. (n = 4, # $p<0.05$; * $p<0.001$).(b) Representative mosaic image showing re-epithelialization at day 7, 9 and 11 after 8 X 16mm wounding. Scale bar = 500µm (c) Immunohistochemical localization of Dicer in the wound edge epidermis. The sections were counter stained with DAPI (blue). The dermal (der) and epidermal (epi) junction is indicated by a dashed white line in each panel. Scale bar = 20 µm.

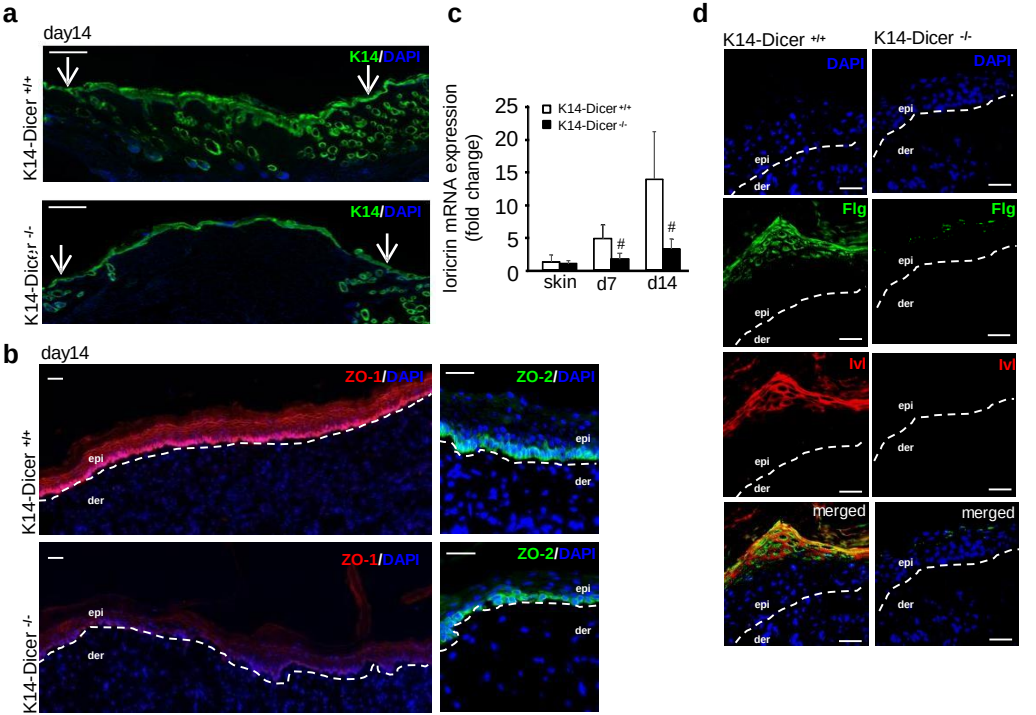

Figure S2: (a) Representative mosaic image from serial wound cross-sections shows K14 immunocytochemistry, counterstained with DAPI, at day 14 post-wounding from three independent experiments. White arrows indicate wound edges. Scale bar = 200µm (b) Representative image from serial wound cross-sections shows ZO-1 mosaic and ZO-2 immunocytochemistry counterstained with DAPI, at day 14 post-wounding from three independent experiments. Scale bar = 50µm (c) Quantitative PCR analysis of loricrin at D0 (skin), day 7 and day 14 wound edge tissue. (n=4,# $p<0.05$).(d) Representative photograph from wound cross-sections showing filaggrin and involucrin co- localization, counterstained with DAPI, at day 14 post-wounding from three independent experiments. The dermal (der) and epidermal (epi) junction is indicated by a dashed white line in each panel. Scale bar = 20 µm

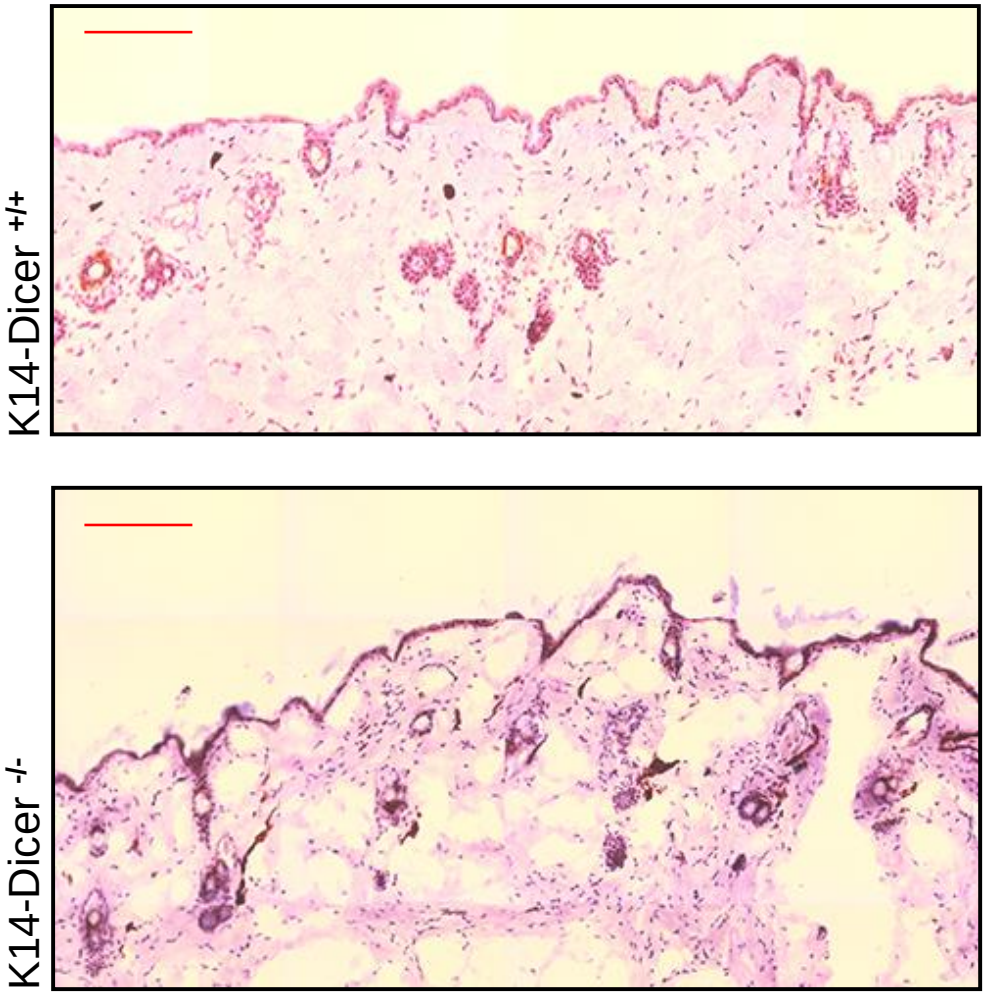

Figure S3: Representative mosaic image of the skin from control and Dicer ablated mice showing immunohistochemical localization of $p21^{waf1/Cip1}$ in the epidermis. Counter staining was performed using hematoxylin. Scale bar = 200µm

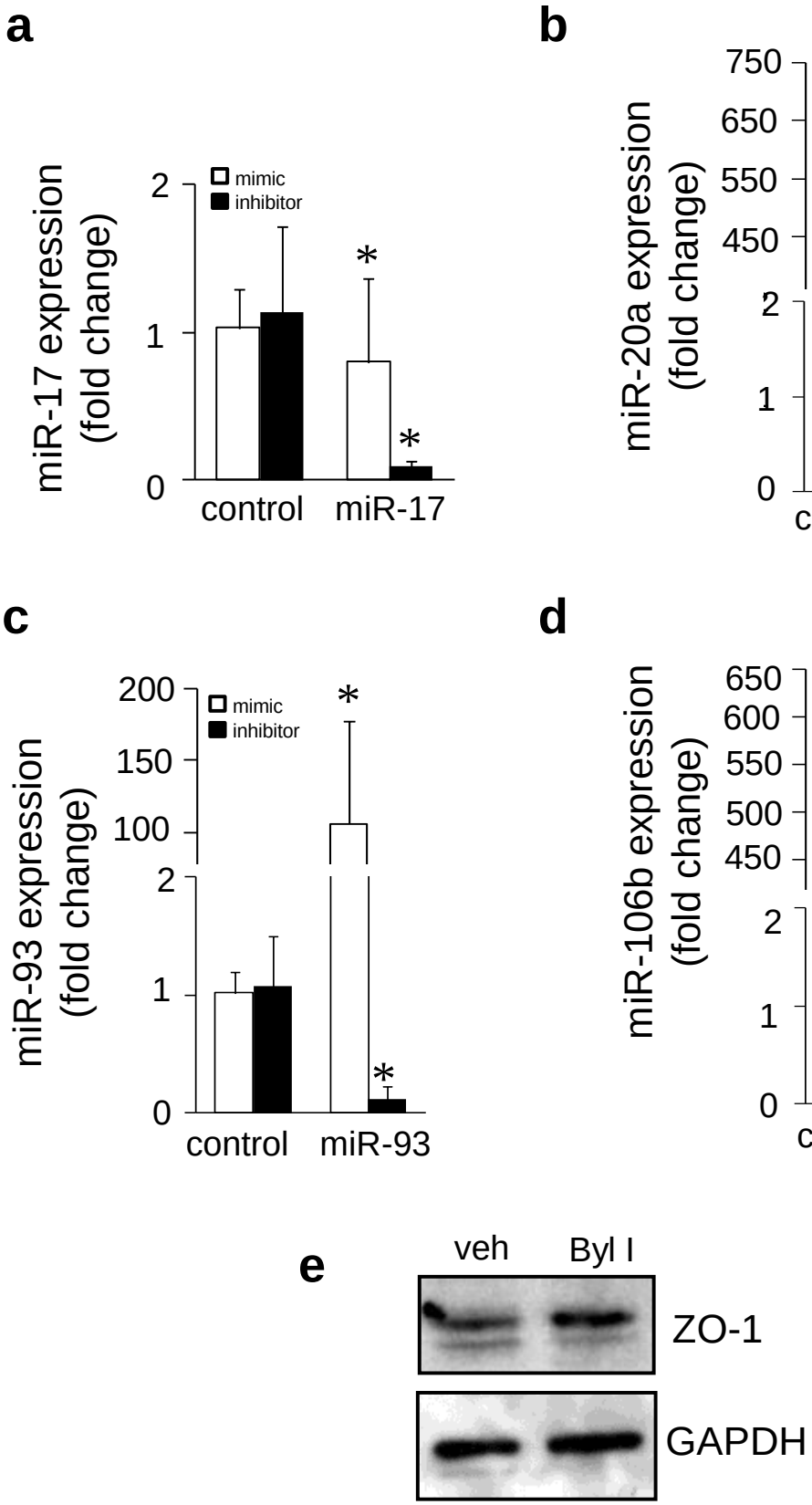

Figure S4: Quantitative PCR analysis of (a) miR-17 (b) miR-20a (c) miR-93 and (d) miR-106b after delivery of mimic and inhibitor respectively. Data expressed as mean ± SD (n=4). * $p<0.001$.(e) Representative Western blot of ZO-1 in HaCaT cells 24h after treatment with p21 inhibitor Butyrolactone I.

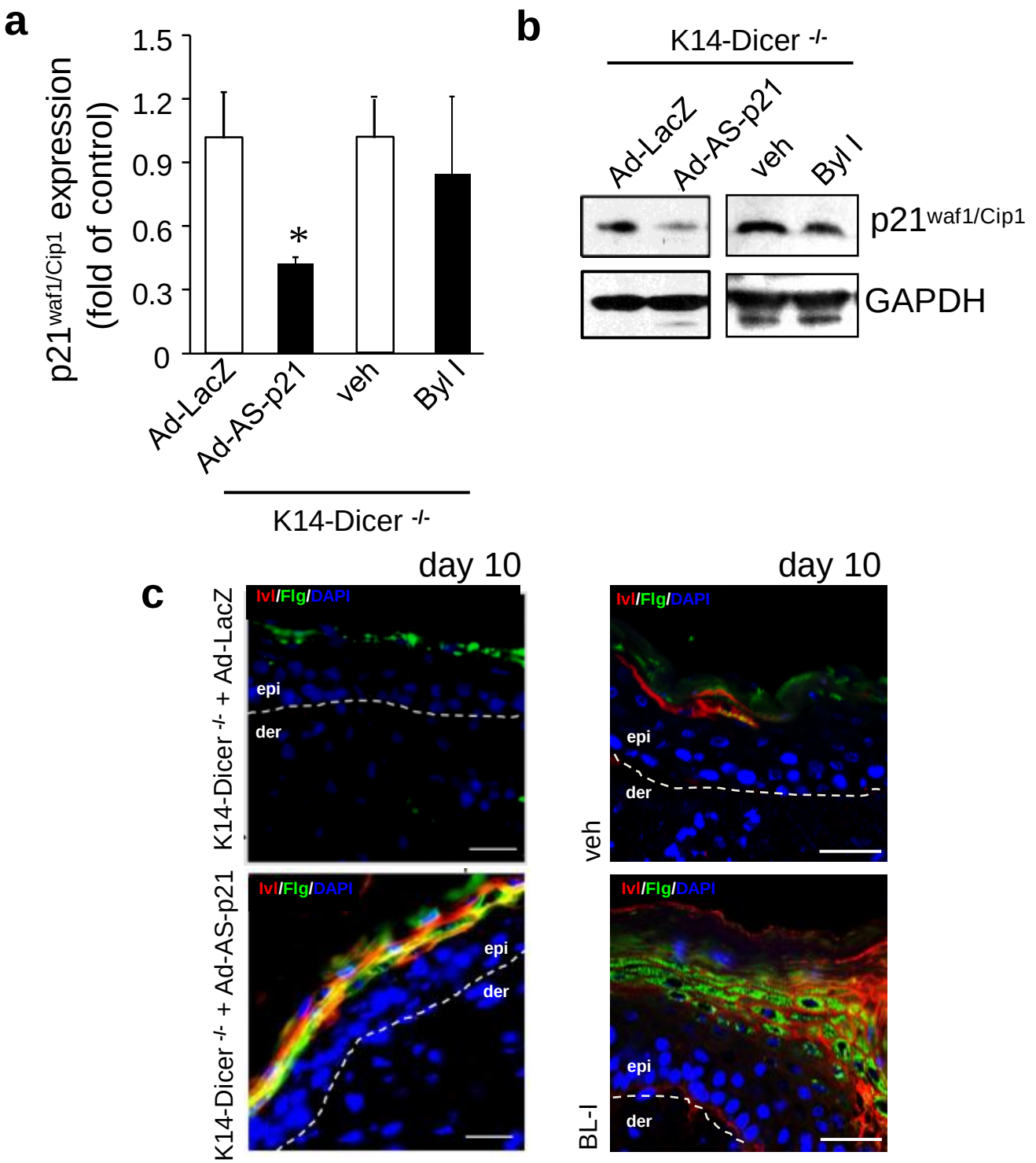

Figure S5: (a) Quantitative PCR analysis and (b) Western blot of p21$^{waf1/Cip1}$ from the wound edge tissue at day 10 post wounding after treating with adeno viral and Butyrolactone I (pharmacological inhibitor of p21$^{waf1/Cip1}$). The quantification of the signal was normalized against GAPDH and the results were expressed as fold induction compared with that of controls. Data were expressed as mean ± SD (n = 3; * $p < 0.001$). (c) Representative photograph of wound cross-sections showing filaggrin and involucrin co-localization, counterstained with DAPI, at day 10 post-wounding from three independent experiments. The dermal (der) and epidermal (epi) junction is indicated by a dashed white line in each panel. . Scale bar = 20 µm

Supplement table 1.

Primer		Sequence	Accession No
m-GAPDH	Forward	5’- GTGCAGTGCCAGCCTCGTCC-3’	NM_008084
	Reverse	5’- GCACCGGCCTCACCCCATTT-3’	
m-Dicer	Forward	5’- ACACGCTCTGGAGAGGTCACCATAT-3’	NM_148948
	Reverse	5’- TCCAAAGTGCCGGAGTCATTAA-3’	
m-p21	Forward	5’- ACAGGAGCAAAGTGTGCCGTTGT-3’	NM_007669
	Reverse	5’- GCTCAGACACCAGAGTGCAAGACA -3’	
m-Loricrin	Forward	5’- ACGGAGGCGGTTCTAGCGGT-3’	NM_008508
	Reverse	5’- GCCCCCTCCGTAGCTCTGCT-3’	
h-GAPDH	Forward	5’- TGACGCTGGGGCTGGCATTG-3’	NM_002046
	Reverse	5’- GCTCTTGCTGGGGCTGGTGG-3’	
h-p21	Forward	5’- GGGTCGAAAACGGCGGCAGA-3’	NM_078467
	Reverse	5’- GGGGGCGGCCAGGGTATGTA-3’	
h-Loricrin	Forward	5’- TGGTGGCTGCGGCTTCTTCG-3’	NM_000427
	Reverse	5’- GCCCCCACCGCTGGAGAAAC-3’	